J. Phase Equilib. Diffus.
https://doi.org/10.1007/s11669-024-01113-y

REVIEW

Advances in CALPHAD Methodology for Modeling Hydrides: A Comprehensive Review

M. Palumbo[1] · E. M. Dematteis[1] · L. Fenocchio[2] · G. Cacciamani[2] · M. Baricco[1]

Submitted: 28 December 2023 / in revised form: 16 April 2024 / Accepted: 18 April 2024

Abstract Hydrides enable handling hydrogen at low pressure and near room temperature, offering higher volumetric densities than compressed or liquid hydrogen and enhancing safety. The CALPHAD method, rooted in the principles of thermodynamics, offers a systematic approach for predicting phase equilibria and thermodynamic properties in multicomponent materials. This comprehensive review paper aims to provide a detailed overview of the application of the CALPHAD method in the realm of metallic and complex hydrides. After an introduction to the fundamental thermodynamic aspects of hydrides, key elements of applying the CALPHAD method to model metal-hydrogen systems and complex hydrides are discussed. Subsequently, recent publications are reviewed, highlighting key findings and recent progresses in the field. Finally, the challenges that must be overcome to achieve further progress in this area are explored.

Keywords CALPHAD · hydrides · hydrogen storage · thermodynamics

This invited article is part of a special tribute issue of the *Journal of Phase Equilibria and Diffusion* dedicated to the memory of Thaddeus B. "Ted" Massalski. The issue was organized by David E. Laughlin, Carnegie Mellon University; John H. Perepezko, University of Wisconsin–Madison; Wei Xiong, University of Pittsburgh; and JPED Editor-in-Chief Ursula Kattner, National Institute of Standards and Technology (NIST).

✉ M. Palumbo
mauro.palumbo@unito.it

[1] Department of Chemistry and NIS- INSTM, University of Turin, V. P. Giuria 7, 10125 Turin, Italy

[2] Dipartimento di Chimica e Chimica Industriale, Università di Genova, Genoa, Italy

1 Introduction

To effectively limit the rise in global temperatures from climate change, it is essential to find alternatives to fossil fuels in transportation and energy production. Renewable energy sources like solar, wind, and water are promising, especially if we can store their energy efficiently. Hydrogen, as an energy carrier, offers several benefits. It is a secondary energy vector, because it is produced from primary energy sources and can be stored for extended periods. Hydrogen is appealing because it reacts with oxygen to produce only water, releasing a significant amount of energy. For instance, 1 kg of hydrogen has the same energy content as 2.4 kg of methane or 2.8 kg of gasoline.[1] This makes hydrogen more energy-dense by weight compared to other fuels. However, its energy density by volume is lower, as evidenced by liquid hydrogen, which contains 8.5 MJ/L compared to 32.6 MJ/L for gasoline. This means a larger volume of hydrogen is needed to match the energy provided by most fossil fuels.

Green hydrogen can be produced through various methods, such as electrolysis, biogas reforming, or photoelectrochemical processing. It can be converted back into energy using fuel cells or internal combustion engines. Utilizing hydrogen as an energy carrier requires the development of a suitable infrastructure for its handling, including purification to remove contaminants, transportation, storage, and compression.

Typically, hydrogen is stored as a compressed gas or cryogenic liquid, technologies which require substantial energy for compression and cooling, making them economically challenging. Alternatively, suitable carriers allow for handling hydrogen at low pressure and near room temperature, offering higher volumetric densities than compressed or liquid hydrogen and enhancing safety.[2] For

Published online: 10 May 2024

example, metallic hydrides are promising materials that can reversibly uptake and release hydrogen and possess a great potential for a wide range of applications.[3–5] Research in the hydrogen sector aims to increase energy density while limiting system volume.

To harness the full potential of metallic hydrides, a deep understanding of their thermodynamic and kinetic properties is essential.[3,6–8] In this context, the CALPHAD (Calculation of Phase Diagrams) method has emerged as a powerful and suitable tool for modeling and predicting the behaviour of hydride systems.[9,10]

The CALPHAD method, rooted in the principles of thermodynamics, offers a systematic approach to the prediction of phase equilibria and thermodynamic properties in multicomponent materials.[11,12] Originally developed in the 1970 s for applications in metallurgy, CALPHAD has since evolved and found wide-ranging utility in diverse fields, including the study of hydrides.[9,10] By combining thermodynamic databases, experimental data, and computational techniques, the CALPHAD approach allows researchers to unravel the complex interplay of phases and reactions that occur during hydrogen absorption and desorption in metallic systems.

This comprehensive review paper aims to provide a detailed overview of the application of the CALPHAD method in the realm of metallic and complex hydrides. We will explore the fundamental concepts behind CALPHAD and its adaptation to address the unique challenges posed by hydride systems. Furthermore, we will delve into the critical contributions of CALPHAD in elucidating the thermodynamics of hydrogen absorption and desorption processes and the design of new hydride materials. Additionally, we will highlight recent advances and future prospects in the field, showcasing the continuous evolution of CALPHAD as an indispensable tool for advancing the science and technology of hydrides. Through this review, we hope to offer researchers, engineers, and materials scientists a comprehensive resource for understanding the state-of-the-art in CALPHAD-based modeling of metallic hydride systems and inspire further advancements in this field.

2 Hydrogen Absorption

Solid hydrogen carriers need to have a substantial mass and volume capacity, along with rapid gas absorption and release rates. Moreover, the hydrogenation reaction should ideally occur near ambient pressures and temperatures. Achieving these characteristics requires appropriate thermodynamic and kinetic properties, as well as optimal gravimetric and volumetric densities for the hydrogen carrier.

On the one hand, the interaction between hydrogen gas (H_2) and a solid-phase carrier (M), typically a metal, can lead to the formation of a solid solution M(H). This process is described by the following reaction:

$$M + \frac{x}{2}H_2 \rightleftarrows M(H) \quad \text{(Eq 1)}$$

In this case, the process is driven by the Sievert law:

$$\frac{H}{M} = K_s p^{1/2} \quad \text{(Eq 2)}$$

where H/M is the ratio between hydrogen and the metal M in the solution, K_s is a constant and p is the pressure. The dependence of K_s on the temperature, T, can be expressed as:

$$\ln K_s = \frac{-\Delta H_{mix}}{RT} + \frac{\Delta S_{mix}}{R} \quad \text{(Eq 3)}$$

where R is the gas constant and ΔH_{mix} and ΔS_{mix} are the partial enthalpy and entropy of mixing, respectively.

On the other hand, the reaction between H_2 and M can lead to the formation of a hydride MH_x, whose crystal structure can be different from that of the parent M:

$$M + \frac{x}{2}H_2 \rightleftarrows MH_x + Q \quad \text{(Eq 4)}$$

where Q is the heat absorbed or released during the reaction. Hydrogen sorption affects the crystal structure and volume of the carrier. During hydride formation (absorption), the crystal structure of M changes to that of MH_x and usually results in a volume increase. Conversely, the volume decreases during desorption.

The thermodynamics of the reaction can be described by the so-called Pressure-Composition-Isotherm (PCI) curves, in which the equilibrium pressure (p_{eq}) is measured as a function of hydrogen content (H/M) at different temperatures. In the two-phase region, where M(H) and MH_x coexist, p_{eq} is related to temperature according to the Van't Hoff equation:

$$\ln p_{eq} = \frac{-\Delta H_{for}}{RT} + \frac{\Delta S_{for}}{R} \quad \text{(Eq 5)}$$

where ΔH_{for} and ΔS_{for} are the enthalpy and entropy of formation of the hydride, respectively. From this reaction, the changes in enthalpy and entropy for both absorption and desorption reactions can be experimentally determined. This is achieved by plotting the natural logarithm of the equilibrium pressure ($\ln p_{eq}$) against the reciprocal of the temperature ($1/T$), in what is known as the Van't Hoff plot.

The composition of the solid solution and the hydride in equilibrium conditions can be established from the knowledge of the free energy of both phases as a function of H/M at constant pressure and temperature, as shown in Fig. 1(a). If this trend can be defined at various

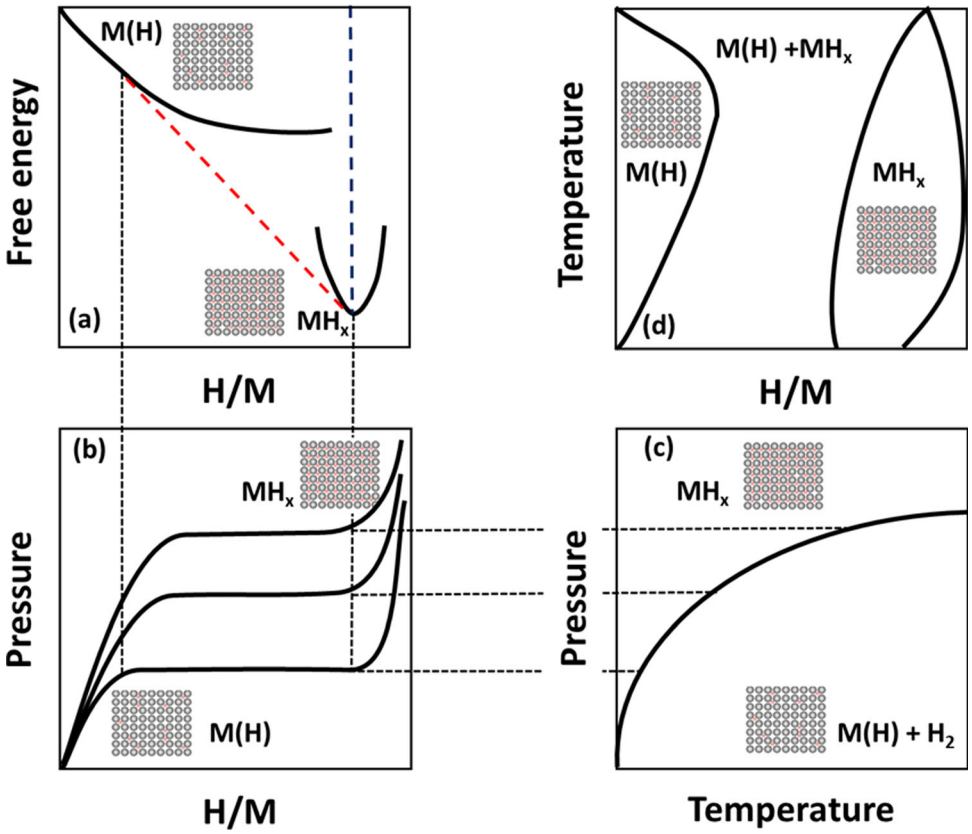

Fig. 1 Graphical representation of the stability of a hydride in terms of free energy, pressure, temperature and composition: (a) free energy of a solid solution, M(H), and a hydride, MH_x, as a function of H/M for constant temperature and pressure; (b) Pressure-Composition-Isotherm (PCI) curves; (c) pressure as a function of temperature at constant composition; (d) phase diagram at constant pressure. In figure (a), the red dashed line shows the common tangent, defining the equilibrium compositions between the hydride and the solid solution of hydrogen in the carrier, and the dashed blue line represents the free energy of formation of the hydride.

temperatures and pressures, the PCI curves can be drawn, as shown in Fig. 1(b). When ΔH_{for} and ΔS_{for} are known as a function of temperature, the equilibrium conditions at constant composition can be established, as shown in Fig. 1(c). Finally, from the knowledge of all the thermodynamic parameters, the phase diagram can be drawn, as shown in Fig. 1(d).

In an ideal scenario, the PCI curves for both absorption and desorption in hydrogen storage systems would display similar trends. However, in real systems, the plateau pressures for absorption and desorption differ, with absorption typically exhibiting higher pressures, indicative of a hysteresis effect. This hysteresis is associated with various sample characteristics, such as preparation conditions and microstructure. It can be managed through specific post-synthesis treatments or by using certain additives. Minimizing hysteresis is important for applications that demand high reversibility and efficiency without losses.

Furthermore, the pressure plateau in PCI diagrams should be flat under full equilibrium conditions, but it can sometimes display a slope. This can be due to impurities, fluctuations in stoichiometry, or para-equilibrium phenomena.[9,13] Again, appropriate treatments or additives can be used to mitigate this slope. Additionally, some materials might exhibit multiple plateaus at different hydrogen-to-metal (H/M) ratios, reflecting the formation of various hydride phases.[14]

The kinetics of hydrogen sorption reactions in hydrogen carriers is crucial for the efficiency of handling systems. These reactions typically involve several steps: physisorption of hydrogen at the surface, dissociation into atoms (chemisorption), diffusion into the carrier, and the formation of a solid solution or hydride through nucleation and growth processes. The reverse process occurs during desorption. Identifying the rate-limiting step, whether it is hydride formation at the interface or a diffusion-based mechanism, is essential for understanding these reactions.

Various approaches, such as the Avrami model and its variations, are used to describe experimental kinetic data. These models are particularly useful in isobaric measurements under isothermal conditions to track hydrogen uptake or release. The reaction rate is temperature-dependent, following the Arrhenius relation. A key parameter is the activation energy (E_a), which indicates the energy barrier for the sorption process. Methods like the Kissinger method, often based on thermal analysis results, are often employed to determine E_a.

The microstructure of the materials significantly influences absorption and desorption rates.[15] Materials with a fine microstructure show high sorption rates, with grain boundaries acting as nucleation sites for phase

formation.[16] Synthesis and processing methods, such as mechanical alloying, can enhance these kinetics. Additionally, the starting powder particle size and surface area, and certain additives, can improve kinetics by increasing the gas contact surface and reducing the hydride nucleation barrier.

In real applications, factors like material activation, powder compaction, thermal conductivity, and the purity of inlet hydrogen play significant roles. Metal surfaces may be covered by an oxide layer, requiring activation processes at high temperatures and pressures to facilitate hydrogen diffusion. Processes like ball milling can also be used for activation, reducing the oxide layer and modifying the microstructure.

3 Metallic Hydrides

The interaction of hydrogen with pure metals has been a topic of several studies.[17] Considering hydrides of pure metals, MgH_2 is an excellent material for hydrogen storage, but, because of its thermodynamic properties, the equilibrium dehydrogenation temperature is rather high (i.e. around 300 °C under 1 bar of H_2) and the sorption kinetics is undesirably slow. LiH has also great potential given its gravimetric capacity, but its thermodynamic stability has so far precluded practical applications. Another promising elemental metal hydride is aluminium hydride (AlH_3), yet it is hindered by challenges in synthesis and very limited reversibility. Other pure metal hydrides also encounter significant barriers: some require extreme conditions for hydrogen sorption reactions (e.g. Ti, Zr), while others have very high costs (e.g. Pd).

In the periodic table, elements that form stable hydrides (AH_y), such as left-side transition metals or rare earth metals, are categorized as element A. In contrast, element B encompasses those that form unstable hydrides (BH_w), typically found among the right-side transition metals. For hydrogen handling with carriers, the stability of hydrides is crucial, because, if it is too high, the hydrogen sorption process becomes irreversible under practical conditions. Intermetallic compounds obtained combining A and B elements demonstrated interesting properties for hydrogen handling. In fact, the resulting $A_mB_nH_z$ hydrides display intermediate properties, combining aspects of both AH_y and BH_w. Favourable stoichiometries, including AB, AB_2, and AB_5, lead to the formation of metal hydrides that efficiently absorb and release hydrogen under nearly ambient temperature and pressure.

A wide array of intermetallic compounds has been explored for hydrogen handling. The most notable AB compound in this context is TiFe, along with its variants achieved by substituting Ti or Fe with other metals. AB_2 compounds typically feature Ti and/or Zr as the A-type element and a transition metal as B. These compounds generally possess Laves-phase crystal structures, such as the hexagonal $MgZn_2$-type (C14), cubic $MgCu_2$-type (C15), and hexagonal $MgNi_2$-type (C36). These structures show several advantages, including high gravimetric capacity, rapid kinetics in absorption and desorption, and an easy activation. However, their resistance to gas impurities is limited due to potential reactions with constituent elements. Various body-centred cubic solid solutions with AB_2 composition have also been identified as promising for hydrogen handling. AB_5 compounds, involving rare earth metals and transition metals, are exemplified by $LaNi_5$. This composition is known for its quick activation, high reversibility at low temperatures, fast kinetics, good resistance to gas impurities, and suitable cycling stability. More recently, High-Entropy Alloys (HEAs) have been proposed for hydrogen storage. These alloys contain elements with varying affinities for hydrogen, leading to promising gravimetric capacities and sorption reactions that occur at temperatures close to normal ambient conditions. A more in-depth discussion of the latest results on HEAs for hydrogen storage can be found in several recent review papers.[18–21]

In the search for effective solid-state hydrogen carriers, complex hydrides have gained attention due to their lightweight nature and high hydrogen-to-metal atom ratio.[6] These hydrides are generally represented by the chemical formula $C_xD_yH_z$, where C elements are typically light elements from the first and second groups of the periodic table, forming the cation. The D element, which forms the complex anion with hydrogen, can be Aluminium, Boron, Nitrogen, or a transition metal.

Alanates, consisting of complex anions like $[AlH_4]^-$ or $[AlH_6]^{3-}$ and their corresponding metal cations, are salt-like, insulating materials. Their theoretical gravimetric capacities vary depending on the metal cation, with notable examples being up to 10.5 wt.% for $LiAlH_4$, 5.5 wt.% for $NaAlH_4$, 5.7 wt.% for $KAlH_4$, and 9.3 wt.% for $Mg(AlH_4)_2$. Borohydrides, another category of inorganic ionic compounds, also serve as suitable hydrogen carriers. For instance, $LiBH_4$ has the highest hydrogen content among metal borohydrides at 18.5 wt.%, while $NaBH_4$, KBH_4, $Mg(BH_4)_2$, and $Ca(BH_4)_2$ have respective contents of 10.7 wt.%, 7.5 wt.%, 14.9 wt.%, and 11.6 wt.%. Amides and imides of alkali and alkaline-earth metals are also potential candidates for hydrogen storage. Furthermore, the development of Reactive Hydride Composites (RHCs), which are mixtures of metal hydrides and complex hydrides (primarily borohydrides or amide/imide), offers a promising approach. These RHCs facilitate reversible hydrogen desorption/absorption that is both kinetically and

thermodynamically favourable under moderate temperature and hydrogen pressure conditions.

4 The CALPHAD Method and Its Application to Hydrogen Absorption in Hydrides

At its core, the CALPHAD method relies on the Gibbs energy minimization. For a given system and set of conditions, the method looks for the equilibrium state (or states), i.e. the minimum of the overall Gibbs energy. This is achieved by representing the Gibbs energy of each possible phase in the system as a function of temperature, pressure, and composition by using specific thermodynamic models. These functions contain empirical parameters whose values need to be determined. These parameters are derived from experimental data, first-principles calculations, or a combination of both in a procedure called "thermodynamic assessment" or "thermodynamic optimization" of the system.

The general formulation of the molar Gibbs energy of a phase φ is given by[11]:

$$G_m^{\varphi} = G_{ref}^{\varphi} + G_{phys}^{\varphi} + G_{conf}^{\varphi} + G_{ex}^{\varphi} \quad \text{(Eq 6)}$$

where G_{ref}^{φ} is the Gibbs free energy of the unreacted mixture of the components, G_{phys}^{φ} is the contribution to Gibbs free energy due to a physical model (e.g. for describing magnetic transitions), G_{conf}^{φ} is the contribution to Gibbs free energy due to the configurational entropy (ideal mixing) and G_{ex}^{φ} is "excess" contribution to Gibbs free energy. Each term can depend on temperature, pressure and composition. The latter term includes all contributions not accounted for in the previous terms and its specific formulation is model dependent. Several models have been developed within the CALPHAD approach and can be chosen to adequately describe the thermodynamics of different phases.[11,12]

Complex multi-phase and multicomponent systems modeling by CALPHAD method requires:

1. Software Tools: several software packages have been developed to exploit CALPHAD calculations. They allow users to input system conditions (like temperature and composition) and obtain predicted phase equilibria, other thermodynamic properties and phase diagrams. They also allow to perform the thermodynamic assessment of the system.
2. Thermodynamic Assessment: this is the process of optimizing the parameters in the Gibbs energy functions. It involves a careful analysis of experimental data, selection of appropriate models for different phases, and iterative optimization to achieve the best fit. The optimization is performed by fitting the interaction parameters to the experimental data (and/or first-principles results) and ensuring consistency across different phases and systems.
3. Thermodynamic Databases: central to the CALPHAD method is the use of thermodynamic databases. These databases generally contain optimized parameters for the two- and three-components subsystems, allowing extrapolations of the Gibbs energy functions in the multicomponent systems to predict their phase equilibria and thermodynamic properties.

Once a thermodynamic database is available, CALPHAD software can be used to compute phase diagrams and estimate the stability of all the phases in the system, also including the hydrides.

The application of the CALPHAD method to M-H systems has steadily been progressing for the past decades in parallel to experimental studies in the hydrogen storage research. One extensive review on M-H systems has been published in 2012 by Joubert et al.[9] and updated three years later.[10] However, after the appearance of these reviews several new systems have been assessed and published in the literature. The periodic table in Fig. 2 shows all the M-H systems for which a thermodynamic assessment has been published. It is noteworthy that, with respect to a similar table presented in,[10] now important systems such as Cr-H, Mn-H and Y-H are available.

Furthermore, it has been previously emphasized that complex hydrides are of interest for hydrogen storage applications, yet these were not included in the two preceding reviews. Table 1 provides an updated version of Table 1 from Joubert's review,[9] where the newly assessed systems, encompassing both intermetallic compounds and complex metallic hydrides, are listed. In the last column, key points pertinent to each system are concisely summarized. Despite the growing interest on HEAs as hydrogen storage materials, the CALPHAD method has been only used to design their base compositions without including the modeling of hydrogen absorption/desorption, hydride formation and their thermodynamics.[22–24]

5 CALPHAD Modeling of Gas, Liquid and Solid Phases in M-H Systems and Hydrides

5.1 The Gas Phase

A proper modeling of the gas phase is of course of paramount importance to reliably describe the thermodynamics of M-H systems and hydrides, particularly in view of

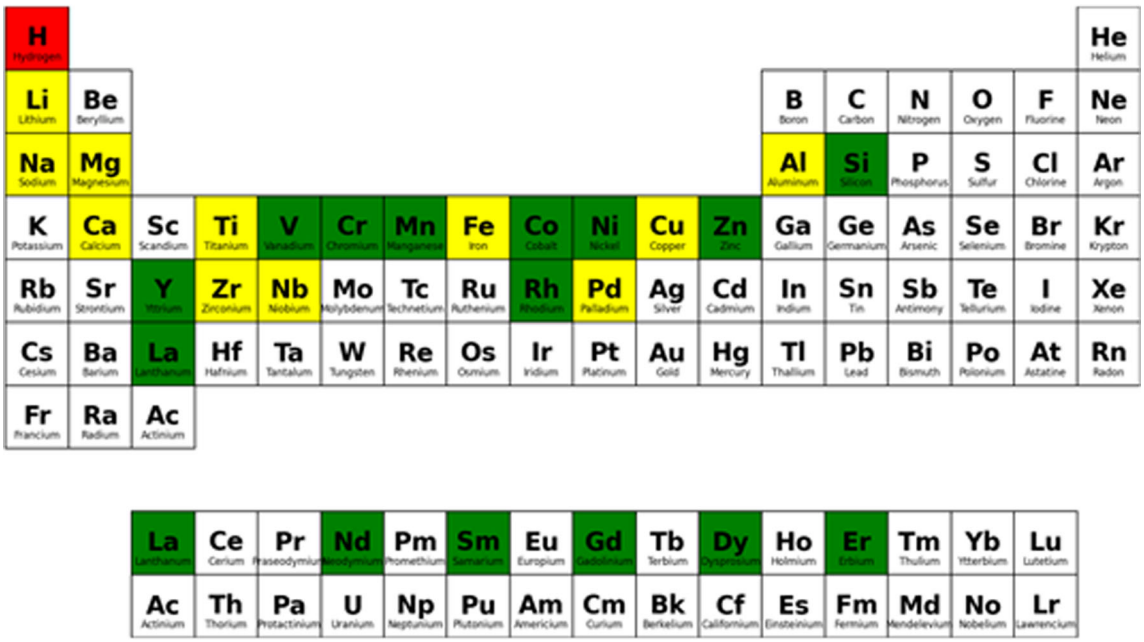

Fig. 2. Periodic table showing the elements for which at least one binary M-H thermodynamic assessment using the CALPHAD method is available. For elements in green, one assessment is available; for elements in yellow, more than one assessment is available.

applying the CALPHAD approach to hydrogen storage applications.

First, the gas phase is generally composed of several species in equilibrium, including biatomic H_2 molecules, but typically containing other species such as monoatomic H, volatile metals (Al, Ca, Li, etc.) and in some cases more species. The presence of different components in the gas phase is described considering ideal mixing among them. This approach is satisfactory as in many cases the amount of these species (except H_2) is so low that their inclusion in the mixture is irrelevant.[9] In fact, in many studies they are simply neglected. This also reflects the typical way experiments of adsorption/desorption are carried out, i.e. in an atmosphere where the presence of other species than H_2 is avoided as much as possible, typically using several steps of purging. However, we remark that the presence of significant amounts of impurities can still be correctly described as long as they behave as an ideal mixture.

Secondly, it is important to adopt a reliable thermodynamic description of the Gibbs free energy of H_2 gas as a function of temperature and pressure. In nearly all published works, it is considered an ideal gas and hence its free energy is

$$G_{H_2}^{gas} = \int V dP = \int \frac{RT}{P} dP = G_{H_2}^{gas} + RTln\left(\frac{P}{P_0}\right) \qquad \text{(Eq 7)}$$

In fact, hydrogen behaves ideally in most practical circumstances, but this may fail at high pressures ($>10^8$ Pa).[51] For example, in applications of hydrogen storage compounds with fuel cells, the operating pressures are well below this value and the operating temperatures are from room temperature to a few hundred degrees. However, in compressors this may not be the case and departure from ideal behaviour could become relevant. Attempts to model the non-ideal behaviour of hydrogen gas have been published in the literature in at least two papers: Bohmhammel et al.[52] have described the temperature dependence at constant pressure of the non-ideal volume (the difference between the ideal and real volume) using a virial approach; on the contrary, Joubert[51] used a different model to describe the pressure dependence at constant temperature of the non-ideal volume. To date, however, these models have found limited applications in CALPHAD assessments (Ni-H,[32] Mg-H,[52] Rh-H[51]). We remark that during the assessment procedure, the necessity of using a non-ideal model for H_2 gas depends on the experimental data used in the process. If these data have been obtained at high pressures, then a proper model for the non-ideal behaviour of H_2 gas must be adopted. This is the case in a recent assessment of the Cr-H system by Dottor et al.[25]. Nonetheless, in nearly all cases the ideal model works fine, and this is by far the most adopted approach.

5.2 The Liquid Phase

The most used model for the liquid phase in CALPHAD assessments of binary systems is arguably the substitutional model with Redlich-Kister polynomials describing the excess contribution to the Gibbs energy.[11] These are

Table 1. CALPHAD assessments of M-H systems, intermetallic compounds and complex hydrides

System	Reference	Notes
Cr-H	[25]	SL model for liquid. Solubility of H in bcc with 2-SL model. Hydrides as stoichiometric compounds. Special model for the gas phase at high pressures. New experimental data
Dy-H	[26]	No liquid. SL model for hydrides. New experimental data
Er-H	[27]	No liquid. SL model for hydrides. New experimental data
Gd-H	[28]	No liquid. SL model for hydrides. New experimental data
Mn-H	[29]	More gas species included (Mn, H). Substitutional model (R-K) for the liquid phase. SL model for solid solution and hydrides: $(Mn)(H,Va)_n$ n = 1 for αMn, βMn, γMn; n = 3 for δMn.
Nb-H	[30]	More gas species included (H, Nb). No liquid. SL models used for solid solutions (hcp, bcc, fcc, fct) and binary hydride NbH. DFT calculations used. New experimental data
Nd-H	[31]	More gas species included (Nd, H). Substitutional model (R-K) for the liquid phase. SL model for NdH_2
Ni-H	[32]	SL model for liquid. Includes the high pressure hydride NiH described with 2-SL model. Special model for the gas phase at high pressures. New DFT data
Y-H	[33]	No liquid. Same 3-SL model, $(Y)(H,Va)(H,Va)_2$, for all hydrides. New experimental data
Y-H	[34]	No liquid. Same 3-SL model, $(Y)(H,Va)(H,Va)_2$, for all hydrides
Zr-H	[35]	No liquid. SL model for hydrides. DFT for end-member energies
Al-RE-H	[36]	Extrapolation from the binaries. RE = Er, La, Y. Focus on the liquid phase. New experimental data.
FeTi-H	[37]	Assessment of the pseudo-binary FeTi-H. The intermetallic compound FeTi is considered as an "element". Introduction of a 'FT' element to account for para-equilibrium conditions during the optimization. SL models for solid solution α and hydrides. New experimental and DFT data
La-Ni-H	[38]	Assessment similar to Ref. [39] except that the ternary hydride $LaNi_5H_7$ is treated both with SL model and as stoichiometric compound. New experimental data
Li-Si-H	[40]	More gas species included (Li, Li_2, Si, etc.). Substitutional model (R-K) for the liquid phase. LiH hydride included as stoichiometric. New experimental data
Mg-Mn-H	[29]	More gas species included (Mn, H). Substitutional model (R-K) for the liquid phase. SL model for ternary hcp solid solution. Stoichiometric model for hydrides Mg_3MnH_6 and Mg_3MnH_7
Nb-Zr-H	[30]	More gas species included (H, Nb, Zr, Zr_2 ZrH). Only binary Nb-Zr liquid. SL models used for solid solutions (hcp, bcc, fcc, fct). No ternary hydrides. DFT calculations used. New experimental data.
Nd-Ni-H	[31]	More gas species included (Nd, H). Substitutional model (R-K + Muggianu) for the liquid phase. Two SL models for $NdNi_5H_3$ and $NdNi_5H_6$. New experimental data
Ti-Zr-H	[41]	A CALPHAD model for the ternary system is mentioned, but no details are given. It is unclear if it is a new assessment or just refers to an earlier publication by Ukita et al. [42]
Y-Zr-H	[34]	No liquid. No ternary hydrides. Extrapolation from binary assessments
Al-La-Ni-H	[13]	Substitutional model (R-K + Muggianu) for the liquid phase. SL model $(La)_1(Ni,Al)_5(H,Va)_7$. DFT for estimating end-member energies. New experimental data
Mg-Nd-Ni-H	[43]	More gas species included (Nd, Mg, H). Substitutional model (R-K + Muggianu) for the liquid phase. SL models for hydrides. New experimental data
$LiBH_4$	[44]	An assessment of the thermodynamic functions for different polymorphs of $LiBH_4$. Ideal gas including H_2, H, B_2 and other species. Liquid phase described as a function of T at constant composition. Ternary hydrides $Li_2B_{12}H_{12}$ and $Li_2B_{10}H_{10}$ included. New DFT data
$LiBH_4$-$NaBH_4$	[45]	Assessment of the pseudo-binary $LiBH_4$- $NaBH_4$.
$LiBH_4$-$NaBH_4$-KBH_4	[46]	Assessment of the pseudo-binary $LiBH_4$-$NaBH_4$, $LiBH_4$-KBH_4, and $NaBH_4$-KBH_4 systems
$LiBH_4$-LiCl	[47]	Assessment of the pseudo-binary $LiBH_4$-LiCl. Description of the phase diagram resulting from Cl^- substituting $(BH_4)^-$ group in $LiBH_4$
$LiBH_4$-LiBr	[48]	Assessment of the pseudo-binary $LiBH_4$-LiBr. Description of the phase diagram resulting from Br^- substituting $(BH_4)^-$ group in $LiBH_4$
$LiBH_4$-LiI	[49]	Assessment of the pseudo-binary $LiBH_4$-LiI. Description of the phase diagram resulting from I^- substituting $(BH_4)^-$ group in $LiBH_4$

Table 1. continued

System	Reference	Notes
$Mg(BH_4)_2$	[50]	An assessment of the thermodynamic functions for different polymorphs of $Mg(BH_4)_2$. Ideal gas including H_2, H, B_2 and other species. No liquid. Ternary hydrides $MgB_{12}H_{12}$ and $Mg(B_3H_8)_2$ included. New DFT data

The list contains only systems that were not reported in the previous review by Joubert [9]. For older assessments, refer to Table I in Ref. [9]. R-K stands for Redlich-Kister polynomial for the excess contribution, SL stands for sublattice and DFT stands for Density Functional Theory. The notes contain the most important points for each publication, and the adopted model for H_2 gas when it is treated as non-ideal.

polynomials of different orders that can be tailored to suitably describe the complex behaviour of the Gibbs energy of the liquid phase as a function of composition. However, this is typically done in metal-metal systems where the interactions among the atoms in the liquid are expected to be close to a regular solution. For other liquid phases, such as those of oxides, the ionic interactions can require specific models. For M-H system, H atoms in the liquid are expected to behave in a significantly different way from metals. Hence, several models have been used in the literature to describe the Gibbs free energy of the liquid phase in M-H systems,[9] including the substitutional model, the 2-sublattices (SLs) model, the associate model and the quasi-chemical model.

It is also noteworthy that there is no widely accepted description for the liquid phase of pure hydrogen. Knowledge of the free energy of the different phases of pure elements is necessary to carry out a CALPHAD assessment of a binary or higher order system. Suitable free energy functions are typically taken from the PURE database, which is an electronic version of an earlier publication by Dinsdale[53] available in all major CALPHAD software packages such as Thermo-Calc, FactSage, Pandat and OpenCalphad[54–57] (with a few changes with respect to the printed version). The free energy of the liquid phase of pure hydrogen is not included in this database. Hence, different versions from different authors have been proposed in the literature from binary assessments and there is no consensus on which one should be adopted.

The usage of different models in the published assessments and of different descriptions for the Gibbs free energy of pure liquid hydrogen makes it difficult to build a common thermodynamic database. In fact, when assembling a database from different subsystems the same model should be adopted for the same phase to maintain self-consistency. This may require the partial reassessment of some subsystems during this step. An example is the assessment of the ternary Al-Mg-H system.[58] The binary subsystems used in this work are from Qiu et al.[59] for the binary Al-H system and Zeng et al.[60] for the binary Mg-H system. Consequently, the thermodynamic parameters for the liquid hydrogen phase differ between the binary aluminium-hydrogen (Al–H) and the magnesium-hydrogen (Mg–H) systems. To maintain consistency in the ternary Al-Mg-H system, the Gibbs free energy parameters for liquid hydrogen from the Al–H system have been retained and a partial reassessment of the Mg–H system has been conducted, focusing exclusively on experimental data related to the liquid phase. This reassessment was performed to establish a new, consistent set of parameters for the liquid phase in this system. A list of available parameters for the Gibbs energy of pure liquid hydrogen is reported in Table 2.

In higher order systems such as ternaries, an extrapolation approach must also be adopted. Three possible schemes exist to extrapolate the Gibbs energy from binary subsystems into a ternary A-B-C system: Muggianu, Kohler, Toop.[11] The first is the most common one, also in published assessments of M-H systems. In principle, the Toop method can offer some advantages in the case of A-B-H systems, where A and B are metals, as it treats the contributions from the binary subsystems differently and hence it is better suited when one of the constituents (H) behaves very differently from the others (A and B). However, the difference in the extrapolated results is usually small and there are other ways to handle the asymmetry of a ternary system. As already mentioned, the process of building a large database with several subsystems is greatly simplified when using the same model and Muggianu is arguably the most common choice.

5.3 Solid Phases

Modeling of solid phases in the CALPHAD approach should be based on their crystal structure.[61] However, the lack of crystallographic data or the necessity to reduce the model complexity and the number of parameters to be optimized during the assessment can impose the adoption of different models. The Compound Energy Formalism (CEF), a widely accepted framework for solid phases, encompasses various approaches under a unified concept.[11] According to this formalism, a phase can be described as composed of one or more SLs, each occupied by one or more components (typically pure elements). The

Table 2. Gibbs free energy parameters for the liquid hydrogen phase proposed in the literature

Gibbs energy function	System(s)	References
$G_H^{liq} = +8035 + 25*T + 2*T*LN(T) + 0.5*G_{H2}^{SER}$	Al-H	[59]
	Al-Mg-H	[58]
	La-H, La-Ni-H	[39]
	Al-La-Ni-H	[13]
$G_H^{liq} = +20946.25 + 35.31*T + 0.5*G_{H2}^{SER}$	Mg-H, Ni-H, Mg-Ni-H	[60]
	La-H, La-Ni-H	[38]
	Nd-H, Nd-Ni-H	[31]
$G_{Cr:H}^{liq} = G_{Cr}^{liq} + 0.5 * G_{H2}^{SER} - 7.952 * 10^3 + 65.4 * T$	Cr-H	[25]
$G_{Ni:H}^{liq} = G_{Ni}^{liq} + 0.5 * G_{H2}^{SER} + 1.769 * 10^4 + 41.0 * T$	Ni-H	[32]

In some cases (Refs. [40,41,43]) it was not clear which parameters have been used.

Last two lines in the table refer to a hypothetical liquid M:H within a sublattice model (M)(H,Va) adopted for the liquid phase. This is not the Gibbs free energy of pure liquid hydrogen, which in this approach is in fact avoided.

notation to identify a specific SL model uses parentheses for each SL and a subscript number to indicate its stoichiometric coefficient. The element(s) that can occupy the sites in each SL are reported inside the parenthesis.

For example, the notation $(M)(H,Va)_2$ indicates a possible two-SLs model, suitable to describe a metallic fcc solid solution with hydrogen, in which the first SL has multiplicity one and the second has multiplicity two. The first SL is occupied only by atoms of the metal M (assuming a binary system), while the second SL can be occupied by both hydrogen atoms and vacancies (Va). The corresponding Gibbs energy is given by:

$$\begin{aligned} G_m^{\varphi} = {} & y_M^1 y_H^2 G_{M:H}^0 + y_M^1 y_{Va}^2 G_{M:Va}^0 \\ & + RT\left(y_M^1 ln y_M^1 + y_H^2 ln y_H^2 + y_{Va}^2 ln y_{Va}^2\right) \\ & + y_M^1 y_H^2 y_{Va}^2 \sum_{\upsilon} L_{M:H,Va}^{\upsilon}\left(y_H^2 - y_{Va}^2\right)^{\upsilon} \end{aligned} \qquad \text{(Eq 8)}$$

where y_A^i is the site fraction of species A in the SL i, $G_{M:H}^0$ and $G_{M:Va}^0$ are the so called end-member energies and $L_{M:H,Va}^{\upsilon}$ are interaction parameters of order υ accounting for interactions between H atoms and vacancies in the second SL while the first is fully occupied by M atoms. The last sum is over υ and the specific number of necessary interaction parameters ($L_{M:H,Va}^0$, $L_{M:H,Va}^1$, etc.) is case dependent. Each $L_{M:H,Va}^{\upsilon}$ can be temperature dependent. $G_{M:H}^0$ end-member energy refers to the case where the first SL is fully occupied by M atoms and the second by H atoms, forming an MH compound; similarly, $G_{M:Va}^0$ refers to the case where the first SL is fully occupied by M atoms and the second by vacancies, i.e. the pure metal M. We note that the above equation can be simplified since y_M^1 is always equal to one, but we kept this form for clarity.

Increasing the number of SLs in the model, the complexity of the equation expressing the free energy and the number of parameters that needs to be determined during the assessment can become excessive. Even if some parameters (for example end-member energies) can be estimated using DFT calculations,[9,13,30] a compromise is often necessary to make the model manageable.

In case of hydrogen atoms in solid solution phases, they occupy the interstitial sites within the metal lattice because of their small size and the type of chemical bonding. To properly chose the correct SL model, the number of available sites and which ones are filled with H atoms on absorption must be known, which is not always the case. In the common metallic structures (bcc, fcc, hcp), two types of interstitial sites exist, tetrahedral and octahedral; H atoms can preferentially fill one type of sites or both.[17] Furthermore, the limited availability of experimental data for the assessment can significantly limit the complexity of the model that can be used. Another relevant feature of M-H solid solutions is that H-H repulsions can limit the insertion of H atoms into the metallic structure.[9,62] In fact, in many M-H systems, small H-H distances are not observed experimentally, suggesting a minimum H-H distance of 2.1 Å and the existence of a site-blocking effect. For this reason, some authors have chosen a SL model different from what could be expected only based on crystallographic features.[63] This has led to several different SL models applied to hcp, bcc and fcc solid solutions in different publications (Table 1 above and Table II in[9]).

For example, in most fcc solid solutions (e.g. Fe-H, Ni-H, Pd-H), H atoms fill tetrahedral sites and the model (M)(H,Va) described above is suitable for modeling their Gibbs energy. However, this is not the case for some fcc (metastable) solid solutions in the Ti-H, V-H and Zr-H systems, where a $(M)(H,Va)_2$ SL model was adopted because it allows to describe the hydride MH_2.[60] Similar issues arise in hcp solid solutions, for which the following SL models

have been adopted in different systems: $(M)(H,Va)_{0.5}$,[64] (M)(H,Va),[65] and $(M)(H,Va)_1(H,Va)_2$.[26]

Besides solid solutions, a proper thermodynamic model must be applied to hydrides as well, also considering their crystal structure. Hydrides obtained from hydrogenation of bcc, fcc, hcp metals have a crystal structure which is usually related to the original solid solution and depends on which and how interstitial sites are filled by H atoms and on whether the structure is significantly distorted upon absorption. If the crystal structure is relatively undistorted, the same SL model can in principle be applied to describe both the solid solution and the resulting hydride at higher hydrogen concentrations. In this case, the Gibbs energy as a function of hydrogen composition at constant temperature would have a miscibility gap, i.e. two minima corresponding to the hydrogen-poor solid solution and to the hydrogen-rich hydride phase. For example, in modeling the binary Er-H system[27] the same SL model, $(Er)(H,Va)(H,Va)_2$, was applied to describe the hcp solid solution and the ErH_3 hydride, as their crystal structures are very similar. The first SL describes the metallic lattice, the second SL the octahedral interstices and the third SL the tetrahedral interstices. In this case, the same model was also adopted for the fcc solid solution and the ErH_2 hydride. However, in other systems, the hydride is modeled with a different SL model with respect to the solid solution, as its crystal structure can be significantly different as a result of distortions produced by the hydrogen atoms when they fill the interstitial sites.[39] We also remark that the choice of the model for the hydrides is often simplified depending on the availability of data for the assessment and the range of hydrogen content at which the hydride is stable. Several hydrides have no solubility range and a simple stoichiometric model can be applied to describe their Gibbs energy.

5.4 Assessment and Calculations

It has already been pointed out that the assessment procedure (or optimization) is a critical step in the CALPHAD methodology as it is necessary to determine the best values for the parameters in the Gibbs energy models. Experimental data used in this step are of various types, including phase diagram and calorimetric data (enthalpy of formation, reaction enthalpies, heat capacities, etc.). Fig. 3 shows an example of phase boundary experimental data used in the assessment of the La-H binary system.[39] Phase diagram data are determined by applying several well-known techniques (optical and electronic microscopy, X-ray diffraction, Differential Scanning Calorimetry, etc.). The use of such experimental data is well established, and the reader can find more details in.[11,12]

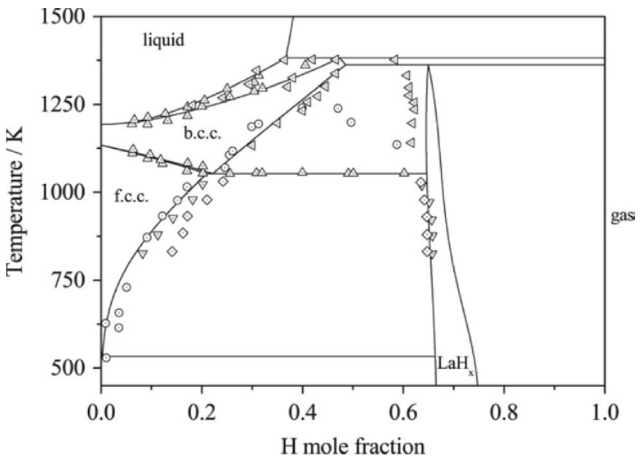

Fig. 3 Calculated (full lines) and experimental (points) phase diagram for the La-H binary system.[39] Reprinted from *Calphad,* Vol 33, M. Palumbo, J. Urgnani, D. Baldissin, L. Battezzati, M. Baricco, Thermodynamic assessment of the H–La–Ni system, Pages No. 162–169, Copyright 2009, with permission from Elsevier

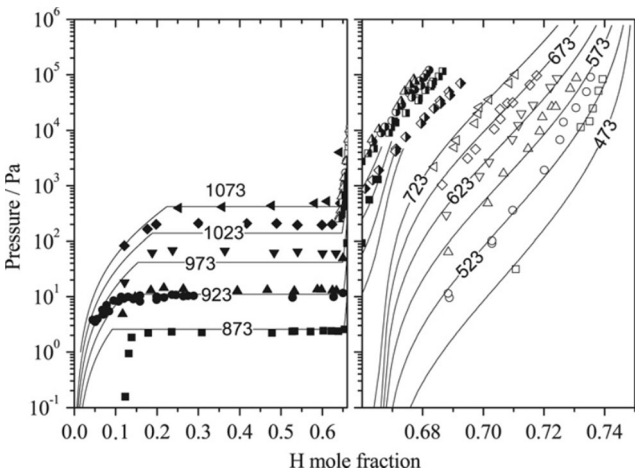

Fig. 4 Calculated PCI curves (full lines) and corresponding experimental data (points) of the La-H binary system. Reprinted from *Calphad,* Vol 33, M. Palumbo, J. Urgnani, D. Baldissin, L. Battezzati, M. Baricco, Thermodynamic assessment of the H–La–Ni system, Pages No. 162–169, Copyright 2009, with permission from Elsevier

A peculiarity of M-H systems is that a very common type of experimental data is the PCI curve, already introduced in a previous section. This type of measurement is used to determine the equilibrium plateau pressure p_{eq} in the biphasic region as a function of H/M at constant temperature, allowing the determination of related phase boundaries. Measurements are typically repeated at various temperatures and Van't Hoff plots are derived. An example of PCI curves is shown in Fig. 4 for the La-H binary system.[39]

Experimental points determined from PCI curves are valuable during the assessment, but some issues arise. In fact, as previously mentioned, it is well known that

experimental PCI curves are not always flat in the biphasic region and in certain systems the slope can be pronounced. If full equilibrium (FE) would be achieved during hydrogen absorption, the related PCI curve should be flat.[66] However, this is not always the case for different reasons.[13] It has been suggested that the presence of a sloped plateau is connected to para-equilibrium (PE) or local equilibrium (LE) conditions.[66] In the first case, the situation can arise in ternary (or higher order) A-B-H systems because of the higher diffusivity of H atoms compared to A/B metal atoms. In this case, the chemical potential of hydrogen can be the same in both phases in the biphasic region, but the chemical potential of the A/B metals is different, i.e. the experimental compositions of A and B in the two phases are not those expected in FE conditions. Another possibility is LE where equilibrium conditions are achieved at the interface between the solid solution and the hydride in the biphasic region, but not necessarily in the rest of the system. A more detailed discussion of these conditions is beyond the scope of this review and the interested reader is referred to Ref. [66]. In a thermodynamic assessment, it is possible to make para-equilibrium or LE calculations under certain conditions, but not during the assessment procedure because of software limitations. There is currently no easy fix for this issue. As a first approximation, for the optimization step FE conditions can be assumed even in systems in which PCI curves show sloped plateau. An a-posteriori check after the assessment can validate this assumption at least in some cases.[13] It is worth noting that in several systems, as for example the La-H system shown in Fig. 3, a flat plateau occurs, and the optimization does not require any special consideration.

Another important point worth discussing related to the use of experimental PCI curves in assessments is the occurrence of hysteresis. A full discussion of this complex phenomenon, which is not limited to hydrogen absorption and desorption, is beyond the scope of this review and the interested reader can refer to Ref..[67] In principle, in a thermodynamic assessment, equilibrium experimental data should be used, though an extension to metastable conditions is possible and sometimes desirable.[39] Hysteresis is a non-equilibrium phenomenon, and it always happens to some extent in hydrogen absorption and desorption reactions.[9,67] The problem, in this case, is that pressure values measured in absorption are different from those measured in desorption for the same system at the same temperature and there is no consensus on whether, in the assessment, values on absorption, desorption or an average between the two should be used. According to Flanagan et al.,[67,68] the average value between absorption and desorption is the closest to thermodynamic equilibrium, and hence it is probably best to input such average in the assessment procedure. However, if data obtained from both absorption and desorption experiments are used during the thermodynamic assessment, the optimization algorithm will consider both, probably leading to a similar result. Even if hysteresis is always present, we remark that only in systems where the phenomenon is pronounced these differences are somewhat relevant in the assessment. In fact, when hysteresis is limited, the difference between absorption and desorption pressures may well fall within the experimental uncertainty of the technique.

We finally remark that the isotope effect is also a peculiarity of thermodynamic assessments involving M-H systems and hydrides. In fact, hydrogen has isotopes (deuterium D and tritium T) which significantly differ in mass from protium (H). For this reason, the thermodynamics of M-H systems can be significantly different from M-D and M-T ones. However, this point has already been discussed exhaustively in Ref. [9], and will not be further considered here, as no significant updates have recently been published.

6 Metal-Hydrogen Systems

As already mentioned, Joubert has reviewed the published assessments for M-H systems in 2012.[9] In particular, Table 1 in his publication reports all the systems for which a thermodynamic assessment has been performed until the publication date. Several new binary M-H systems have been assessed since, as shown in Table 1.

We remark that several RE-H (RE = Rare Earths) systems, well known for forming hydrides, have been assessed in recent years, including Dy-H,[26] Er-H,[27] Gd-H[28] and Y-H.[34] In all these assessments, the gas phase has been described as ideal and the CEF has been adopted for the hydrides. Increasing the number of available binary M-H thermodynamic assessments is certainly promising in view of the creation of a multicomponent database, though some of the above systems may not be particularly interesting for direct applications in hydrogen storage.

Some transition metals/hydrogen systems have also been added to the list of available assessments. Notably, this includes the Mn-H binary system,[29] which is an important subsystem not only for hydrogen storage. The presence of several allotropes of pure Mn, which all can absorb a certain amount of hydrogen in solid solution, and hydrides requires the adoption of different SL models for each phase. Furthermore, this assessment has been extended to the ternary Mg-Mn-H system, including ternary hydrides such as Mg_3MnH_6 and Mg_3MnH_7.

Another important binary system that has been recently assessed is Cr-H.[25] The bcc solid solution between Cr and H is described with a two-SLs model $(Cr)(Va,H)_3$, whereas the hydrides are considered as stoichiometric compounds,

as not enough convincing evidence exists of a possible composition range. An important peculiarity of this assessment is that it includes experimental data at high pressures (up to 18 GPa) where the H_2 gas cannot be considered ideal. Hence the authors have adopted a suitable thermodynamic model, as already mentioned in a previous section. A revision of the Gibbs free energy of pure chromium has also been proposed. DFT calculations were also used for estimating the thermodynamic functions of pure Cr and binary end-members and compounds.

Some additional binary assessments described above have been extended into ternary systems, such as the Nb-Zr-H[30] and Y-Zr-H.[34] Other ternary and quaternary systems assessed will be discussed in the next section focused on intermetallic compounds.

7 Intermetallic Compounds

As already pointed out, some intermetallic compounds form hydrides and have promising properties for hydrogen storage. Some CALPHAD assessments describe the hydrogenation process and the thermodynamics of the systems in which these compounds appear. A first example is the assessment of the La-Ni-H ternary system,[39] which accounts for the hydrogen absorption in the intermetallic compound $LaNi_5$. This compound has suitable properties for hydrogen storage applications and is already used for industrial applications, but its high density makes it unsuitable for mobile applications. In the assessment of the La-Ni-H ternary system, a full assessment of the binary La-H was also carried out as it was missing. The Gibbs energy of LaH_x and $LaNi_5H_x$ hydrides was modeled using SL models and several calorimetric data and PCI measurements were used. We remark that, in this work, the authors have chosen to use the Gibbs free energy parameters for pure liquid hydrogen from their previous work to be consistent and they have hence partially reassessed the Ni-H description from.[60] This work was later extended to the quaternary system Al-La-Ni-H[13] to include the hydrogenation behaviour of $La(Ni,Al)_5$, where partial substitution of Al atoms in $LaNi_5$ can help tailor its thermodynamic properties. DFT calculations were used to estimate the formation energy of some end-members. The influence of para-equilibrium conditions on the calculated results has also been tested and found negligible in this case.

A similar approach has been adopted by Luo et al.[31] in evaluating the ternary Nd-Ni-H system. The Gibbs free energy parameters for pure liquid hydrogen from[39] were adopted, the binary Nd-H was assessed as part of this work and two different SL models were tested for the hydride phases. The work provides a complete description of the thermodynamics of the ternary system investigated and extend the coverage of $NiRE_5$ (RE = Rare Earths) compounds. More recently, a thermodynamic assessment of the quaternary Mg-Nd-Ni-H system has been published,[43] extending the work of.[31] To the best of our knowledge, only two thermodynamic assessments of quaternary systems have been reported, the other one being the already mentioned Al-La-Ni-H. Besides collecting all published experimental data on the system, Li et al.[43] have carried out a full thermodynamic analysis of the ternary Mg-Nd-Ni system, followed by assessment extension to include the hydrogenation behaviour of relevant binary intermetallic compounds such as Mg_2Ni, $NdMgNi_4$ and $NdMg_2Ni_9$. As reported in Table 1, different SL models were adopted for these compounds and the related hydrides, the liquid phase was described with a Redlich-Kister-Muggianu model, and the gas phase as an ideal gas (also containing Mg, Ni and Nd in an ideal mixture).

Another interesting intermetallic compound with RE is $CeNi_2$, which has been experimentally investigated by Di Chio et al.[69] More recently, enthalpy of formation of amorphous hydrides in Ce-Ni-H and its subsystems has been calculated by Liu et al. using the Miedema model,[70] but no full CALPHAD assessment has been reported yet to the best of authors' knowledge.

The main drawback of RE-based compounds is their high density, so that some alternative lighter compounds have been explored. This is the case of the FeTi intermetallic compound, and a recent thermodynamic evaluation of the FeTi-H pseudo-binary phase diagram goes in this direction.[37] Even if this work does not cover the entire composition range of the ternary Fe-Ti-H system, it provides the necessary thermodynamic parameters for describing the hydrogenation of FeTi. Different SL models in the CEF framework have been adopted for the solid solutions and hydrides. The assessment has been carried out with the open-source software OpenCalphad[55] and special emphasis has been placed on the para-equilibrium issue during the assessment discussed in a previous section. Alvares et al. have merged Fe and Ti into a hypothetical element 'FT' and set up the utilized SL models accordingly. For example, the B2-α phase has been described with a two-SLs model $(FT)(Va, H)_3$ where the first SL is fully occupied by the hypothetical element 'FT' and the second SL is filled with vacancies and H atoms. When the second SL is filled only with vacancies, the equimolar FeTi compound is obtained. This approach allowed the authors to perform the thermodynamic assessment under para-equilibrium conditions, but it limits the model to the equimolar composition between Fe and Ti, neglecting its solubility range and limiting the possibility to extend it to the full ternary Fe-Ti-H system and higher order systems.

8 Complex Hydrides

Although complex hydrides have gained significant interest, the number of CALPHAD assessments pertaining to these systems remains limited, primarily because they have only been studied extensively in recent years. However, there are some publications showing promising progress. For example, El Kharbachi et al.[44] and Pinatel et al.[50] have optimized the thermodynamic functions for $LiBH_4$ and $Mg(BH_4)_2$, respectively, including several species in the gas phase and various binary and ternary hydrides. Both these studies also integrate DFT results in the assessment procedure. The thermodynamic database produced was then applied to rationalize the dehydrogenation behaviour of these compounds and possible products. Earlier analysis the thermodynamics of $LiBH_4$,[71] NaH, Na_3AlH_6, $NaAlH_4$,[72] and $NaBH_4$[73] have also been reported.

The $LiBH_4$–$NaBH_4$ pseudo-binary system has been investigated by X-ray diffraction, temperature-programmed photographic analysis, and differential scanning calorimetry, in order to establish the phase diagram.[45] Ab initio calculations have been performed to establish the relative stabilities of the pure compounds in orthorhombic, hexagonal and cubic structures. The formation of solid solutions was confirmed by powder X-ray diffraction measurements performed as a function of temperature. A eutectic composition between $Li_{0.65}Na_{0.35}BH_4$ and $Li_{0.70}Na_{0.30}BH_4$, with a melting temperature of 216 °C, was observed. The obtained experimental and calculated data were compared with available literature values, and they were used for a thermodynamic assessment of the $LiBH_4$–$NaBH_4$ pseudo-binary phase diagram by the CALPHAD method (Fig. 5).

More recently, there has been growing interest in partially substituting the BH_4^- anion in $LiBH_4$ and $Mg(BH_4)_2$ with halogen elements to fine tune the thermodynamic stability of the resulting mixed hydride. Some thermodynamic assessments have been carried out covering this partial substitution of the BH_4^- anion in $LiBH_4$ with halogen elements X = Cl, Br, I.[47] While these evaluations do not encompass the entire compositional range of the quaternary Li-B-H-X system, they successfully reproduce the pseudo-binary $LiBH_4$-LiX phase diagrams, representing the pertinent vertical section of the full quaternary diagram.

9 Applications

Performing a thermodynamic assessment offers the advantage of determining a consistent set of Gibbs energy functions, from which phase diagram and complete thermodynamics of the system can be derived. Consequently,

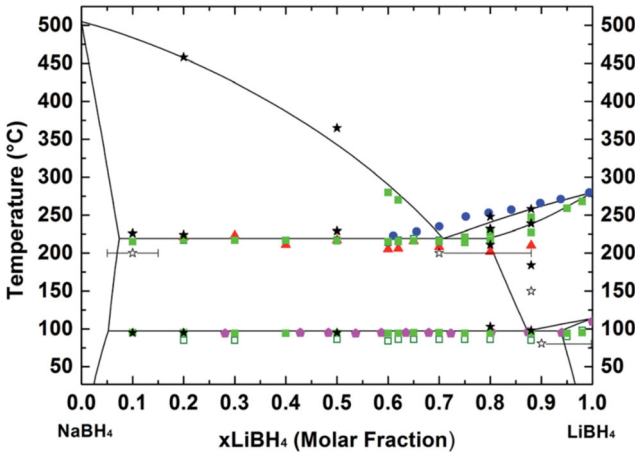

Fig. 5 Pseudo-binary phase diagram of the $LiBH_4$–$NaBH_4$ system. Experimental and literature data (points) are compared with the calculation (lines) from the CALPHAD assessment. Reproduced from Ref. [45] with permission from the Royal Society of Chemistry

the calculated phase diagram is completely consistent with the thermodynamics of the system, which is not always the case when only experimental investigations are considered. It must be noted that the phase diagram is univocally determined by the Gibbs energy functions of the different phases; on the contrary such functions are not univocally determined by the phase equilibria. It follows that a thermodynamic optimization can provide a much clearer insight into the thermodynamic properties of a system, rather than a mere analysis of available experimental data, which is often discrete and fragmented. Furthermore, for hydrides, the CALPHAD method allows the calculation of PCI curves at arbitrary temperatures and the evaluation and comparison of different reaction paths for synthesis and decomposition.

The most crucial feature of the CALPHAD method is the possibility to predict the behaviour of multicomponent systems, once a thermodynamic database is available, containing interaction parameters for all the Gibbs energies of the 2- and 3-component subsystems. This is possible since the Gibbs energy functions for multicomponent systems can be obtained by ideal extrapolation from those of the subsystems, without the addition of new empirical parameters. Unfortunately, such a multicomponent database is not yet available for hydrogen-related systems, as the subsystems have only been partially assessed.

We finally remark that the availability of a multicomponent database for hydrides systems will also open the way to new applications, which are already common for other materials. For example, the use of thermodynamic quantities obtained from CALPHAD calculations is quite common in several kinetic models for describing phase transformations. Additionally, new methodologies based on big data approaches and machine learning can greatly

benefit from the ability to calculate thermodynamic quantities across a wide range of temperatures, pressures, and compositions for various materials. These calculated quantities can be used as predictors or features in machine learning models allowing the construction of large datasets needed in such approaches.

10 Challenges

The number of available assessments for hydride systems remains relatively scarce compared to those for other types of systems, like those critical for steels and other materials. However, the situation is constantly improving as evidenced by the increasing number of CALPHAD assessments reported in recent literature.

A significant challenge in building a multicomponent database for hydrides is the absence of a widely accepted description for the pure hydrogen liquid phase. Though this limitation primarily affects applications involving the liquid phase, which is not the case for hydrogen storage applications, it is desirable to find a standard and accepted description which avoids the necessity of partial reassessments to address consistency.

Similarly, employing different SL models (or other models) for solid solutions and hydrides raises consistency issues in the construction of a multicomponent database. However, it is worth noting that different models have been already applied to systems relevant to steels in the past. On the contrary, this is actually part of the freedom that each author has to apply the model that is considered more suitable for a certain system/phase/application, and in fact the presence of several assessments of the same system applying different models enriches the possibilities offered by the methodology. Nonetheless, when constructing a multicomponent database, it is crucial to ensure that the model applied to each phase remains consistent across all the included systems.

We finally note that the literature additionally presents alternative thermodynamic approaches, which do not fully comply with the distinctive features of the CALPHAD method. For instance, a recent study[74] introduces a thermodynamic strategy for calculating PCT curves under para-equilibrium conditions. This strategy employs a formula that considers the chemical potentials of the metal alloy, the hydride, and the hydrogen gas, akin to a common tangent construction (illustrated by the red dashed line in Fig. 1(a)). These authors do not use any CALPHAD software, but an explicit equation based on chemical potentials; this, allows them to adopt specific and recent models which are not yet implemented in CALPHAD software. One of the advantages, for instance, consists in the appropriate description of the configurational entropy of the hydrides explicitly considering site-blocking effects when hydrogen atoms fill interstitial sites. On the other hand, extending this methodology to include multicomponent equilibria with additional phases, such as other gases or solid phases that may compete with the hydrides and hydrogen gas in terms of thermodynamic stability, presents challenges. Similarly, applying this approach to fully map the phase diagram of these systems would be problematic. In theory, alternative thermodynamic methods like the one proposed in[74] could be integrated into the CALPHAD framework through their implementation in the software or the adoption of already present similar/equivalent models. Such integration is desirable to leverage the advanced multicomponent equilibria calculation algorithms and the extensive thermodynamic databases developed and maintained by the CALPHAD community, enhancing the analysis of several systems documented in the literature.

11 Conclusions

This review thoroughly examines metal-hydrogen systems, including complex hydrides and those derived from intermetallic compounds, through the lens of the CALPHAD approach. The review demonstrates that the thermodynamic evaluation of metal-hydrogen systems exhibits unique characteristics compared to other systems. Additionally, it provides an updated overview of related publications, building upon previously published reviews on the topic. Despite the challenges outlined, the review maintains a positive outlook, suggesting that the advancement of hydrogen storage materials will greatly benefit from the insights gained through thermodynamic calculations within the CALPHAD framework.

Acknowledgments The authors would like to express their deep appreciation for the fruitful inspiration over the years with Ted Massalski. His insightful guidance in research on the thermodynamics of materials has left an indelible impact and will always be remembered with great respect and gratitude. Support from the Project CH4.0 under the MUR program "Dipartimenti di Eccellenza 2023-2027" (CUP: D13C22003520001) is acknowledged. The authors want to acknowledge the EX-MACHINA project leading to this publication, which it has received funding under the MUR program "PNNR M4C2 Initiative 1.2: Young Researcher - Seal of Excellence" (CUP: D18H22002040007). This publication is part of the project NODES which has received funding from the MUR e M4C2 1.5 of PNRR with grant agreement no. ECS00000036.

Funding Open access funding provided by Università degli Studi di Torino within the CRUI-CARE Agreement.

References

1. M. Ball, and M. Wietschel, The Future of Hydrogen – Opportunities and Challenges, *Int. J. Hydrogen Energy*, 2009, **34**, p 615–627. https://doi.org/10.1016/J.IJHYDENE.2008.11.014
2. T. He, P. Pachfule, H. Wu, Q. Xu, and P. Chen, Hydrogen carriers, *Nat. Rev. Mater.*, 2016, **1**(12), p 1–17. https://doi.org/10.1038/natrevmats.2016.59
3. M. Hirscher, V.A. Yartys, M. Baricco, J. Bellosta von Colbe, D. Blanchard, R.C. Bowman, D.P. Broom, C.E. Buckley, F. Chang, P. Chen, Y.W. Cho, J.C. Crivello, F. Cuevas, W.I.F. David, P.E. de Jongh, R.V. Denys, M. Dornheim, M. Felderhoff, Y. Filinchuk, G.E. Froudakis, D.M. Grant, E.M.A. Gray, B.C. Hauback, T. He, T.D. Humphries, T.R. Jensen, S. Kim, Y. Kojima, M. Latroche, H.W. Li, M.V. Lototskyy, J.W. Makepeace, K.T. Møller, L. Naheed, P. Ngene, D. Noréus, M.M. Nygård, S. Ichi Orimo, M. Paskevicius, L. Pasquini, D.B. Ravnsbæk, M. Veronica Sofianos, T.J. Udovic, T. Vegge, G.S. Walker, C.J. Webb, C. Weidenthaler, and C. Zlotea, Materials for Hydrogen-Based Energy Storage – Past Recent Progress and Future Outlook, *J. Alloys Compd.*, 2020, **827**, p 153548. https://doi.org/10.1016/J.JALLCOM.2019.153548
4. A. Züttel, Materials for hydrogen storage, *Mater. Today*, 2003, **6**, p 24–33. https://doi.org/10.1016/S1369-7021(03)00922-2
5. L. Schlapbach, and A. Züttel, Hydrogen-Storage Materials for Mobile Applications, *Nature*, 2001, **414**(6861), p 353–358. https://doi.org/10.1038/35104634
6. E.M. Dematteis, M.B. Amdisen, T. Autrey, J. Barale, M.E. Bowden, C.E. Buckley, Y.W. Cho, S. Deledda, M. Dornheim, P. De Jongh, J.B. Grinderslev, G. Gizer, V. Gulino, B.C. Hauback, M. Heere, T.W. Heo, T.D. Humphries, T.R. Jensen, S.Y. Kang, Y.S. Lee, H.W. Li, S. Li, K.T. Møller, P. Ngene, S.I. Orimo, M. Paskevicius, M. Polanski, S. Takagi, L. Wan, B.C. Wood, M. Hirscher, and M. Baricco, Hydrogen Storage in Complex Hydrides: Past Activities and New Trends, *Progress in Energy*, 2022, **4**, p 032009. https://doi.org/10.1088/2516-1083/AC7499
7. M. Dornheim, L. Baetcke, E. Akiba, J.R. Ares, T. Autrey, J. Barale, M. Baricco, K. Brooks, N. Chalkiadakis, V. Charbonnier, S. Christensen, J. Bellosta Von Colbe, M. Costamagna, E. Dematteis, J.F. Fernandez, T. Gennett, D. Grant, T.W. Heo, M. Hirscher, K. Hurst, M. Lototskyy, O. Metz, P. Rizzi, K. Sakaki, S. Sartori, E. Stamatakis, A. Stuart, A. Stubos, G. Walker, C.J. Webb, B. Wood, V. Yartys, and E. Zoulias, Research and Development of Hydrogen Carrier Based Solutions for Hydrogen Compression and Storage, *Progress in Energy*, 2022, **4**, p 042005. https://doi.org/10.1088/2516-1083/AC7CB7
8. V.A. Yartys, M.V. Lototskyy, E. Akiba, R. Albert, V.E. Antonov, J.R. Ares, M. Baricco, N. Bourgeois, C.E. Buckley, J.M. Bellosta von Colbe, J.C. Crivello, F. Cuevas, R.V. Denys, M. Dornheim, M. Felderhoff, D.M. Grant, B.C. Hauback, T.D. Humphries, I. Jacob, T.R. Jensen, P.E. de Jongh, J.M. Joubert, M.A. Kuzovnikov, M. Latroche, M. Paskevicius, L. Pasquini, L. Popilevsky, V.M. Skripnyuk, E. Rabkin, M.V. Sofianos, A. Stuart, G. Walker, H. Wang, C.J. Webb, and M. Zhu, Magnesium Based Materials for Hydrogen Based Energy Storage: Past, Present and Future, *Int. J. Hydrogen Energy*, 2019, **44**, p 7809–7859. https://doi.org/10.1016/J.IJHYDENE.2018.12.212
9. J.M. Joubert, CALPHAD modeling of Metal-Hydrogen Systems: A Review, *JOM*, 2012, **64**, p 1438–1447. https://doi.org/10.1007/S11837-012-0462-6
10. J.M. Joubert, Thermodynamic Modelling of Metal–Hydrogen Systems Using the Calphad Method, *J. Alloys Compd.*, 2015, **645**, p S379–S383. https://doi.org/10.1016/J.JALLCOM.2014.12.105
11. H.L. Lukas, S.G. Fries, B. Sundman, Computational Thermodynamics: The Calphad Method 9780521868112, 1–313 (2007).https://doi.org/10.1017/CBO9780511804137
12. N. Saunders, and A.P. Miodownik, *CALPHAD (Calculation of Phase Diagrams) - A Comprehensive Guide*, 1st edn. Pergamon Materials Series, London, 1998.
13. E.R. Pinatel, M. Palumbo, F. Massimino, P. Rizzi, and M. Baricco, Hydrogen Sorption in the LaNi5-xAlx-H System ($0 \leq x \leq 1$), *Intermetallics (Barking)*, 2015, **62**, p 7–16. https://doi.org/10.1016/J.INTERMET.2015.03.002
14. T. Tanaka, M. Keita, and D.E. Azofeifa, Theory of Hydrogen Absorption in Metal Hydrides, *Phys. Rev. B*, 1981, **24**, p 1771–1776. https://doi.org/10.1103/PhysRevB.24.1771
15. E. David, An Overview of Advanced Materials for Hydrogen Storage, *J. Mater. Process. Technol.*, 2005. https://doi.org/10.1016/j.jmatprotec.2005.02.027
16. M. Dornheim, S. Doppiu, G. Barkhordarian, U. Boesenberg, T. Klassen, O. Gutfleisch, and R. Bormann, Hydrogen Storage in Magnesium-Based Hydrides and Hydride Composites, *Scr. Mater.*, 2007, **56**, p 841–846. https://doi.org/10.1016/J.SCRIPTAMAT.2007.01.003
17. Y. Fukai, *The Metal-Hydrogen System, Materials Science*. Springer, Berlin, 1992.
18. F. Marques, M. Balcerzak, F. Winkelmann, G. Zepon, and M. Felderhoff, Review and Outlook on High-Entropy Alloys for Hydrogen Storage, *Energy Environ. Sci.*, 2021, **14**, p 5191–5227. https://doi.org/10.1039/D1EE01543E
19. R.R. Shahi, A.K. Gupta, and P. Kumari, Perspectives of High Entropy Alloys as Hydrogen Storage Materials, *Int. J. Hydrogen Energy*, 2023, **48**, p 21412–21428. https://doi.org/10.1016/J.IJHYDENE.2022.02.113
20. L. Kong, B. Cheng, D. Wan, and Y. Xue, A Review on BCC-Structured High-Entropy Alloys for Hydrogen Storage, *Front Mater*, 2023, **10**, p 1135864. https://doi.org/10.3389/FMATS.2023.1135864
21. L. Luo, L. Chen, L. Li, S. Liu, Y. Li, C. Li, L. Li, J. Cui, and Y. Li, High-Entropy Alloys for Solid Hydrogen Storage: A Review, *Int. J. Hydrogen Energy*, 2024, **50**, p 406–430. https://doi.org/10.1016/J.IJHYDENE.2023.07.146
22. R. Floriano, G. Zepon, K. Edalati, G.L.B.G. Fontana, A. Mohammadi, Z. Ma, H.W. Li, and R.J. Contieri, Hydrogen Storage in TiZrNbFeNi High Entropy Alloys, Designed by Thermodynamic Calculations, *Int. J. Hydrogen Energy*, 2020, **45**, p 33759–33770. https://doi.org/10.1016/J.IJHYDENE.2020.09.047
23. P. Edalati, R. Floriano, A. Mohammadi, Y. Li, G. Zepon, H.W. Li, and K. Edalati, Reversible Room Temperature Hydrogen Storage in High-Entropy Alloy TiZrCrMnFeNi, *Scr. Mater.*, 2020, **178**, p 387–390. https://doi.org/10.1016/J.SCRIPTAMAT.2019.12.009
24. G. Andrade, G. Zepon, K. Edalati, A. Mohammadi, Z. Ma, H.W. Li, and R. Floriano, Crystal Structure and hydrogen Storage Properties of AB-Type TiZrNbCrFeNi High-Entropy Alloy, *Int. J. Hydrogen Energy*, 2023, **48**, p 13555–13565. https://doi.org/10.1016/J.IJHYDENE.2022.12.134
25. M. Dottor, J.C. Crivello, and J.M. Joubert, Thermodynamic Modeling of Cr and Cr–H Systems Up to High Temperatures and

High Pressures, *Int. J. Hydrogen Energy*, 2022, **47**, p 23293–23309. https://doi.org/10.1016/J.IJHYDENE.2022.04.245
26. K. Fu, G. Li, J. Li, Y. Liu, W. Tian, and X. Li, Experimental Study and Thermodynamic Assessment of the Dysprosium-Hydrogen Binary System, *J. Alloys Compd.*, 2017, **696**, p 60–66. https://doi.org/10.1016/J.JALLCOM.2016.11.182
27. A. Mascaro, C. Toffolon-Masclet, C. Raepsaet, and J.M. Joubert, Experimental Study and Thermodynamic Assessment of the Erbium–Hydrogen Binary System, *Calphad*, 2013, **41**, p 50–59. https://doi.org/10.1016/J.CALPHAD.2013.01.004
28. K. Fu, G. Li, J. Li, Y. Liu, W. Tian, J. Zheng, and X. Li, Study on the Thermodynamics of the gadolinium-Hydrogen Binary System (H/Gd = 0.0–2.0) and Implications to Metallic Gadolinium Purification, *J Alloys Compd*, 2016, **673**, p 131–137. https://doi.org/10.1016/J.JALLCOM.2016.02.201
29. Y. Liang, S. Liu, and Y. Du, Thermodynamic Assessment of the Mn-H and Mg-Mn-H Systems, *J Phase Equilibria Diffus*, 2018, **39**, p 186–195. https://doi.org/10.1007/S11669-018-0622-7/FIGURES/6
30. M. Dottor, J.C. Crivello, and J.M. Joubert, Critical Reassessment of the H-Nb System and Experimental Investigation and Thermodynamic Modeling of the H–Nb–Zr System, *Calphad*, 2023, **83**, p 102617. https://doi.org/10.1016/J.CALPHAD.2023.102617
31. Q. Luo, S.L. Chen, J.Y. Zhang, L. Li, K.C. Chou, and Q. Li, Experimental Investigation and Thermodynamic Assessment of Nd–H and Nd–Ni–H Systems, *Calphad*, 2015, **51**, p 282–291. https://doi.org/10.1016/J.CALPHAD.2015.10.009
32. N. Bourgeois, J.C. Crivello, A. Saengdeejing, Y. Chen, P. Cenedese, and J.M. Joubert, Thermodynamic Modeling of the Ni-H System, *J. Phys. Chem. C*, 2015, **119**, p 24546–24557. https://doi.org/10.1021/ACS.JPCC.5B06393
33. K. Fu, X. Jiang, Y. Guo, S. Li, J. Zheng, W. Tian, and X. Li, Experimental Investigation and Thermodynamic Assessment of the Yttrium-Hydrogen Binary System, *Prog. Nat. Sci. Mater. Int.*, 2018, **28**, p 332–336. https://doi.org/10.1016/J.PNSC.2018.04.001
34. J. Peng, M. Wu, F. Du, F. Yang, J. Shen, L. Wang, X. Ye, and G. Yan, Thermodynamic Modelling of Y-H and Y–Zr–H System Aided by First-Principles and Its Application in Bulk Hydride Moderator Fabrication, *J. Nucl. Mater.*, 2020, **531**, p 152035. https://doi.org/10.1016/J.JNUCMAT.2020.152035
35. Y. Zhong, and D.D. MacDonald, Thermodynamics of the Zr–H Binary System Related To Nuclear Fuel Sheathing and Pressure Tube Hydriding, *J. Nucl. Mater.*, 2012, **423**, p 87–92. https://doi.org/10.1016/J.JNUCMAT.2012.01.016
36. J. Prigent, J.M. Joubert, and M. Latroche, Study of the Ternary System Al–H–RE (RE = Er, La and Y) in Liquid State, *Int. J. Hydrogen Energy*, 2017, **42**, p 22348–22352. https://doi.org/10.1016/J.IJHYDENE.2017.01.002
37. E. Alvares, P. Jerabek, Y. Shang, A. Santhosh, C. Pistidda, T.W. Heo, B. Sundman, and M. Dornheim, Modeling the Thermodynamics of the FeTi Hydrogenation Under Para-Equilibrium: An ab-initio and Experimental Study, *Calphad*, 2022, **77**, p 102426. https://doi.org/10.1016/J.CALPHAD.2022.102426
38. X.H. An, Q.F. Gu, J.Y. Zhang, S.L. Chen, X.B. Yu, and Q. Li, Experimental Investigation and Thermodynamic Reassessment of La–Ni and LaNi5–H Systems, *Calphad*, 2013, **40**, p 48–55. https://doi.org/10.1016/J.CALPHAD.2012.12.002
39. M. Palumbo, J. Urgnani, D. Baldissin, L. Battezzati, and M. Baricco, Thermodynamic Assessment of the H-La–Ni System, *Calphad*, 2009, **33**, p 162–169. https://doi.org/10.1016/J.CALPHAD.2008.09.003
40. S.M. Liang, F. Taubert, A. Kozlov, J. Seidel, F. Mertens, and R. Schmid-Fetzer, Thermodynamics of Li-Si and Li-Si-H Phase Diagrams Applied to Hydrogen Absorption and Li-Ion Batteries, *Intermetallics (Barking)*, 2017, **81**, p 32–46. https://doi.org/10.1016/J.INTERMET.2017.02.024
41. G. Deng, X. Zhao, S. Wang, X. Liu, Z. Li, and L. Jiang, Characterization of Ti-Based Hydrogen Absorbing Alloys, *Int. J. Hydrogen Energy*, 2013, **38**, p 13050–13054. https://doi.org/10.1016/J.IJHYDENE.2013.03.094
42. S. Ukita, H. Ohtani, and M. Hasebe, Thermodynamic Analysis of the Ti-Zr-H Ternary Phase Diagram, *Adv Mat Res*, 2007, **26–28**, p 989–992. https://doi.org/10.4028/WWW.SCIENTIFIC.NET/AMR.26-28.989
43. Q. Li, Q. Luo, and Q.F. Gu, Insights into the Composition Exploration of Novel Hydrogen Storage Alloys: Evaluation of the Mg–Ni–Nd–H Phase Diagram, *J. Mater. Chem. A Mater.*, 2017, **5**, p 3848–3864. https://doi.org/10.1039/C6TA10090B
44. A. El Kharbachi, E. Pinatel, I. Nuta, and M. Baricco, A Thermodynamic Assessment of LiBH4, *Calphad*, 2012, **39**, p 80–90. https://doi.org/10.1016/J.CALPHAD.2012.08.005
45. E.M. Dematteis, E. Roedern, E.R. Pinatel, M. Corno, T.R. Jensen, and M. Baricco, A Thermodynamic Investigation of the LiBH4–NaBH4 System, *RSC Adv.*, 2016, **6**, p 60101–60108. https://doi.org/10.1039/C6RA09301A
46. E.M. Dematteis, E.R. Pinatel, M. Corno, T.R. Jensen, and M. Baricco, Phase Diagrams of the LiBH4–NaBH4–KBH4 System, *Phys. Chem. Chem. Phys.*, 2017, **19**, p 25071–25079. https://doi.org/10.1039/C7CP03816J
47. O. Zavorotynska, M. Corno, E. Pinatel, L.H. Rude, P. Ugliengo, T.R. Jensen, and M. Baricco, Theoretical and Experimental Study of LiBH4-LiCl Solid Solution, *Crystals*, 2012, **2**, p 144–158. https://doi.org/10.3390/CRYST2010144
48. V. Gulino, E.M. Dematteis, M. Corno, M. Palumbo, and M. Baricco, Theoretical and Experimental Studies of LiBH4-LiBr Phase Diagram, *ACS Appl. Energy Mater.*, 2021, **4**, p 7327–7337. https://doi.org/10.1021/ACSAEM.1C01455
49. A. Mazzucco, E.M. Dematteis, V. Gulino, M. Corno, M.F. Sgroi, Palumbo M., Baricco M., Experimental and theoretical studies of the LiBH4-LiI phase diagram (2023)
50. E.R. Pinatel, E. Albanese, B. Civalleri, and M. Baricco, Thermodynamic Modelling of Mg(BH4)2, *J. Alloys Compd.*, 2015, **645**, p S64–S68. https://doi.org/10.1016/J.JALLCOM.2015.01.199
51. J.M. Joubert, A Calphad-Type Equation of State for Hydrogen Gas and Its Application to the Assessment of Rh–H System, *Int. J. Hydrogen Energy*, 2010, **35**, p 2104–2111. https://doi.org/10.1016/J.IJHYDENE.2010.01.006
52. K. Bohmhammel, U. Wolf, G. Wolf, and E. Königsberger, Thermodynamic Optimization of the System Magnesium–Hydrogen, *Thermochim. Acta*, 1999, **337**, p 195–199. https://doi.org/10.1016/S0040-6031(99)00235-X
53. A.T. Dinsdale, SGTE Data for Pure Elements, *Calphad*, 1991, **15**, p 317–425. https://doi.org/10.1016/0364-5916(91)90030-N
54. J.O. Andersson, T. Helander, L. Höglund, P. Shi, and B. Sundman, Thermo-Calc & DICTRA, Computational Tools for Materials Science, *Calphad*, 2002, **26**, p 273–312. https://doi.org/10.1016/S0364-5916(02)00037-8
55. B. Sundman, U.R. Kattner, M. Palumbo, and S.G. Fries, OpenCalphad—A Free Thermodynamic Software, *Integr. Mater. Manuf. Innov.*, 2015. https://doi.org/10.1186/s40192-014-0029-1
56. C.W. Bale, E. Bélisle, P. Chartrand, S.A. Decterov, G. Eriksson, A.E. Gheribi, K. Hack, I.H. Jung, Y.B. Kang, J. Melançon, A.D. Pelton, S. Petersen, C. Robelin, J. Sangster, P. Spencer, and M.A. Van Ende, FactSage Thermochemical Software and Databases, 2010–2016, *Calphad*, 2016, **54**, p 35–53. https://doi.org/10.1016/J.CALPHAD.2016.05.002
57. S.L. Chen, S. Daniel, F. Zhang, Y.A. Chang, X.Y. Yan, F.Y. Xie, R. Schmid-Fetzer, and W.A. Oates, The PANDAT Software

Package and Its Applications, *Calphad*, 2002, **26**, p 175–188. https://doi.org/10.1016/S0364-5916(02)00034-2
58. M. Palumbo, F.J. Torres, J.R. Ares, C. Pisani, J.F. Fernandez, and M. Baricco, Thermodynamic and Ab Initio Investigation of the Al–H–Mg System, *Calphad*, 2007, **31**, p 457–467. https://doi.org/10.1016/J.CALPHAD.2007.04.005
59. C. Qiu, G.B. Olson, S.M. Opalka, and D.L. Anton, Thermodynamic Evaluation of the Al-H System, *J. Phase Equilib. Diffus.*, 2004, **25**, p 520–527. https://doi.org/10.1007/S11669-004-0065-1/METRICS
60. K. Zeng, T. Klassen, W. Oelerich, and R. Bormann, Critical Assessment and Thermodynamic Modeling of the Mg–H System, *Int. J. Hydrogen Energy*, 1999, **24**, p 989–1004. https://doi.org/10.1016/S0360-3199(98)00132-3
61. R. Ferro, and G. Cacciamani, Remarks on Crystallochemical Aspects in Thermodynamic Modeling, *Calphad*, 2002, **26**, p 439–458. https://doi.org/10.1016/S0364-5916(02)00056-1
62. D.G. Westlake, Site Occupancies and Stoichiometries in Hydrides of Intermetallic Compounds: Geometric Considerations, *J. Less Common Metals*, 1983, **90**, p 251–273. https://doi.org/10.1016/0022-5088(83)90075-9
63. M. Zinkevich, N. Mattern, A. Handstein, and O. Gutfleisch, Thermodynamics of Fe–Sm, Fe–H, and H-Sm Systems and Its Application to the Hydrogen–Disproportionation–Desorption–Recombination (HDDR) Process for the System Fe17Sm2–H2, *J. Alloys Compd.*, 2002, **339**, p 118–139. https://doi.org/10.1016/S0925-8388(01)01990-9
64. K.H. Kim, J.H. Shim, and B.J. Lee, Effect of Alloying Elements (Al Co, Fe, Ni) on the Solubility of Hydrogen in Vanadium: A Thermodynamic Calculation, *Int. J. Hydrogen Energy*, 2012, **37**, p 7836–7847. https://doi.org/10.1016/J.IJHYDENE.2012.01.117
65. E. Königsberger, G. Eriksson, and W.A. Oates, Optimisation of the Thermodynamic Properties of the Ti–H and Zr–H Systems, *J. Alloys Compd.*, 2000, **299**, p 148–152. https://doi.org/10.1016/S0925-8388(99)00816-6
66. T.B. Flanagan, and W.A. Oates, Some Thermodynamic Aspects of Metal Hydrogen Systems, *J. Alloys Compd.*, 2005, **404–406**, p 16–23. https://doi.org/10.1016/J.JALLCOM.2004.11.108
67. T.B. Flanagan, and H. Noh, Thermodynamics and Hysteresis for Hydrogen Solution and Hydride Formation in Pd-Ni Alloys, *Zeitschrift für Naturforschung – Sect. A J. Phys. Sci.*, 1995, **50**, p 475–486. https://doi.org/10.1515/ZNA-1995-4-522
68. T.B. Flanagan, and W.A. Oates, The Palladium-Hydrogen System, *Annu. Rev. Mater. Sci.*, 1991, **21**, p 269–304. https://doi.org/10.1146/annurev.ms.21.080191.001413
69. M. Di Chio, S. Livraghi, and M. Baricco, Hydrogen Absorption–Desorption in CeNi2, *J. Alloys Compd.*, 2006, **426**, p 180–185. https://doi.org/10.1016/J.JALLCOM.2006.02.041
70. Z. Liu, F. Ruan, Y. Li, T. Zhai, M. Zhao, and J. Zhang, Modeling of Amorphous Phase Formation and its Thermodynamic Behaviour in CeMgH, CeNiH and MgNiH, *Intermetallics (Barking)*, 2019, **105**, p 79–91. https://doi.org/10.1016/J.INTERMET.2018.10.026
71. Y.W. Cho, J.H. Shim, and B.J. Lee, Thermal Destabilization of Binary and Complex Metal Hydrides by Chemical Reaction: A Thermodynamic Analysis, *Calphad*, 2006, **30**, p 65–69. https://doi.org/10.1016/J.CALPHAD.2005.10.002
72. B.M. Lee, J.W. Jang, J.H. Shim, Y.W. Cho, and B.J. Lee, Thermodynamic Assessment of the NaH ↔ Na3AlH6 ↔ NaAlH4 Hydride System, *J. Alloys Compd.*, 2006, **424**, p 370–375. https://doi.org/10.1016/J.JALLCOM.2006.01.008
73. J. Urgnani, F.J. Torres, M. Palumbo, and M. Baricco, Hydrogen Release from Solid State NaBH4, *Int. J. Hydrogen Energy*, 2008, **33**, p 3111–3115. https://doi.org/10.1016/J.IJHYDENE.2008.03.031
74. G. Zepon, B.H. Silva, C. Zlotea, W.J. Botta, and Y. Champion, Thermodynamic Modelling of Hydrogen-Multicomponent Alloy Systems: Calculating Pressure-Composition-Temperature Diagrams, *Acta Mater.*, 2021. https://doi.org/10.26434/CHEMRXIV.14459313.V1